Atmos. Chem. Phys. Discuss., 15, 5423–5459, 2015
www.atmos-chem-phys-discuss.net/15/5423/2015/
doi:10.5194/acpd-15-5423-2015

Atmospheric Chemistry and Physics Discussions
Open Access

The vertical structure of cloud radiative heating over the Indian subcontinent during summer monsoon

E. Johansson[1], A. Devasthale[1], T. L'Ecuyer[2], A. M. L. Ekman[3,4], and M. Tjernström[3,4]

[1]Atmospheric Remote Sensing, Research and development department, Swedish Meteorological and Hydrological Institute (SMHI), Norrköping, Sweden
[2]Department of Atmospheric and Oceanic Sciences, University of Wisconsin-Madison, Madison, USA
[3]Department of Meteorology, Stockholm University (MISU), Stockholm, Sweden
[4]Bolin Center for Climate Research, Stockholm University, Stockholm, Sweden

Received: 14 January 2015 – Accepted: 27 January 2015 – Published: 25 February 2015

Correspondence to: E. Johansson (erik.johansson@smhi.se)

Published by Copernicus Publications on behalf of the European Geosciences Union.

Abstract

Every year the monsoonal circulation over the Indian subcontinent gives rise to a variety of cloud types that differ considerably in their ability to heat or cool the atmosphere. These clouds in turn affect monsoon dynamics via their radiative impacts, both at the surface and in the atmosphere. New generation of satellites carrying active radar and lidar sensors are allowing realistic quantification of cloud radiative heating (CRH) by resolving the vertical structure of the atmosphere in an unprecedented detail. Obtaining this information is a first step in closing the knowledge gap in our understanding of the role that different clouds play as regulators of the monsoon and vice versa.

Here, we use collocated CloudSat-CALIPSO data sets to understand following aspects of cloud-radiation interactions associated with Indian monsoon circulation. (1) How does the vertical distribution of CRH evolve over the Indian continent throughout monsoon season? (2) What is the absolute contribution of different clouds types to the total CRH? (3) How do active and break periods of monsoon affect the distribution of CRH? And finally, (4) what are the net radiative effects of different cloud types on surface heating?

In general, the vertical structure of CRH follows the northward migration and the retreat of monsoon from May to October. It is found that the alto- and nimbostratus clouds intensely warm the middle troposphere and equally strongly cool the upper troposphere. Their warming/cooling consistently exceeds $\pm 0.2\,\mathrm{K\,day^{-1}}$ (after weighing by vertical cloud fraction) in monthly mean composites throughout the middle and upper troposphere respectively, with largest impact observed in June, July and August. Deep convective towers cause considerable warming in the middle and upper troposphere, but strongly cool the base and inside of the tropical tropopause layer (TTL). Such cooling is stronger during active ($-1.23\,\mathrm{K\,day^{-1}}$) monsoon conditions compared to break periods ($-0.36\,\mathrm{K\,day^{-1}}$). The contrasting warming effect of high clouds inside the TTL is found to be double in magnitude during active conditions compared to break periods.

ACPD

15, 5423–5459, 2015

It is further shown that stratiform clouds (combining alto- and nimbostratus clouds) and deep convection significantly cool the surface with net radiative effect in the order of −100 and −400 $W m^{-2}$, respectively, while warming the atmosphere in the order of 40 and 150 $W m^{-2}$. While deep convection produces strong cooling at the surface during active periods of monsoon, the importance of stratiform clouds, on the other hand, increases during break periods. The contrasting CREs in the atmosphere and at surface, and during active and break conditions, have direct implications for monsoonal circulation.

1 Introduction

Clouds cover about 70 % of the Earth's surface area (Stubenrauch et al., 2012) and are key components of the Earth's energy and water cycle. They have multiple influences on the state of the atmosphere, occurring over a wide range of spatio-temporal scales. From an energy perspective, apart from modulating the net surface radiation, clouds substantially influence the diabatic heat budget of the atmosphere through radiative heating/cooling and latent heat release (Fueglistaler et al., 2009a; L'Ecuyer and McGarragh, 2010). Therefore, they are an important part of the land–ocean–atmosphere coupling mechanisms that regulate atmospheric circulation. The World Climate Research Program (WCRP) has identified the understanding of clouds and their coupling with atmospheric circulation as one of their Grand Challenges (http://www.wcrp-climate.org/index.php/grand-challenges/gc-clouds). Quantifying the role of clouds for the energy budget on shorter time scales (days to months) and the implications and feedbacks on climate on longer time scales (years) is critical to address this challenge.

One region where the multiple effects of clouds on radiation are palpable is the Indian subcontinent, where clouds affect the surface, the lower troposphere, and the upper troposphere (and hence the monsoonal circulation). During pre- to post-monsoon transitioning and intra-seasonal oscillations of precipitation, mesoscale convective sys-

ACPD
15, 5423–5459, 2015

tems give rise to a variety of cloud types that differ considerably in their ability to radiatively heat or cool the atmosphere. The latent heating produced by condensation and freezing processes dominates in the low to midlevel part of the troposphere. The latent heating in concert with cloud radiative heating (CRH) is generally considered to be large enough to sustain monsoonal circulation throughout the summer months (Webster et al., 1998). The role of aerosols in modulating clouds is also important in the atmosphere. Both natural and anothropogenic aerosols contribute to the indirect effects and are in turn processed by clouds. In particular, absorbing aerosols have potency to perturb moist static energy affecting the location and strength of monsoonal convection and hence associated clouds (Wang et al., 2009).

In the upper troposphere, the importance of CRH increases with increasing altitude. Two cloud types, deep convection and isolated ice clouds (esp. thin cirrus), are of paramount importance in the upper troposphere lower stratosphere (UTLS) and the tropical tropopause layer (TTL) (Yang et al., 2010). One of the challenging questions currently being addressed by the scientific community is what role deep convective clouds play in conditioning the UTLS region, especially the TTL (Feldman et al., 2008; Fueglistaler et al., 2009a; Fueglistaler and Fu, 2006; Randel and Jensen, 2013; Yang et al., 2010). Although the net and long-term effect of deep convective clouds may be to dehydrate the TTL, these clouds occasionally penetrate and moisten the TTL. Simultaneously the cooling at the top of deep convection can be quite strong. They may also have contrasting impact just below the bottom of the TTL. Radiatively speaking, the cooling at the top of these clouds could significantly impact the local-scale motions just at the base of the TTL and prevent downward sinking of relatively warmer TTL air. With regard to thin cirrus clouds, there is no consensus on the relative contribution of different processes (e.g. in-situ formation vs. convective origin) leading to their formation (Luo and Rossow, 2004). But their impact on the UTLS region, especially the TTL is widely recognized. For example, it is considered that the large-scale uplift of air masses in the Brewer–Dobson circulation is facilitated in the TTL by the presence of thin cirrus. The net heating effect of these thin clouds could enhance the upwelling and transport

ACPD
15, 5423–5459, 2015

of air masses across the TTL (producing enough slow ascent to dehydrate the TTL). In spite of their importance, the uncertainties in their net radiative effect in the UTLS region are high. This is especially true for the Indian monsoon region, where their impact is most tangible in the summer monsoon months. The role of the Indian monsoon in influencing the composition of UTLS region is also widely recognized (Gettelman et al., 2004; James et al., 2008; Park et al., 2008; Randel and Park, 2006).

Finally, it must be noted that the cloud radiative effects at surface are also quite strong in the Indian subcontinent. As will be shown later, although the magnitude of cloud radiative effect at surface depends strongly on the cloud type and cloud microphysical properties, the net total cloud radiative effect is to cool the surface. This negative net radiative effect is spatially variable over the subcontinent and the high frequency of optically thick clouds is largely responsible for such cooling. It is also to be noted that this is contrary to the atmospheric cloud radiative effect, which remains largely positive throughout the core monsoon months and helps drive the circulation. The cloud radiative effect at surface could further influence active and break periods of monsoon. The strong cooling at surface caused by persistent optically thick clouds could suppress the convection in the following days, thus helping induce break in monsoon conditions.

In spite of this pivotal role played by clouds in impacting monsoon and modulating the energy budget over the Indian subcontinent, our understanding of their radiative heating/cooling effects is clearly inadequate. Quantifying detailed vertical structure of CRH over this region has remained especially difficult. One of the main reasons behind the limited knowledge on CRH has been the lack of suitable observations of the vertical structure of the atmosphere. As a result, there exist significant differences in CRH estimates amongst various reanalyses (Ling and Zhang, 2013; Wright and Fueglistaler, 2013) as well as between models and observations (McFarlane et al., 2007). The A-Train constellation of satellites is an extremely useful and indispensable source of information in this context, providing detailed observations of the vertical structure of key atmospheric as well as of surface components, required to estimate CRH (L'Ecuyer and Jiang, 2010; Henderson et al., 2013). Here we use the state-of-the-art estimates

ACPD
15, 5423–5459, 2015

of CRH for the years 2006–2011 derived from the application of broadband radiative transfer calculations to cloud and aerosol information derived from space based lidar and radar data (L'Ecuyer et al., 2008; Henderson et al., 2013) to partially close the knowledge gap in this field of research. We specifically seek to answer the following scientific questions.

1. How does the vertical distribution of CRH evolve over the Indian continent during pre-monsoon, monsoon and post-monsoon seasons?
2. What is the absolute contribution of different clouds types to the total CRH?
3. How do active and break periods of monsoon affect the distribution of CRH?
4. What are the net radiative effects of different cloud types at surface?

The first three questions are discussed with specific focus on the UTLS region.

2 Data and methodology

For the present study we used retrievals of radiative heating/cooling profiles from the 2B-FLXHR-LIDAR product that exploits synergy from the sensors onboard the A-Train convoy of satellites, especially from the Cloud Profiling Radar onboard CloudSat and Cloud-Aerosol Lidar with Orthogonal Polarization onboard Cloud-Aerosol Lidar and Infrared Pathfinder Satellite Observations (CALIPSO) satellites (L'Ecuyer et al., 2008; Henderson et al., 2013). The detailed algorithm theoretical basis for retrievals is explained here: http://www.cloudsat.cira.colostate.edu/ICD/2B-FLXHR-LIDAR/2B-FLXHR-LIDAR_PDICD.P_R04.20111220.pdf.

The retrieval algorithm uses a broadband two-stream plane-parallel doubling-adding radiative transfer model consisting of six shortwave and twelve longwave bands. For each atmospheric layer, the information on state variables (temperature, humidity, ozone etc.) is obtained from ECMWF (ERA-Interim), and cloud and aerosol properties are obtained from the various CloudSat and CALIPSO products. For example,

ACPD
15, 5423–5459, 2015

2B-GEOPROF-LIDAR product (Mace et al., 2008) provides time and location of cloud layers, while 2B-CWC (Cloud Water Content), 2B-TAU (Cloud optical depth) and 2B-PRECIP-COLUMN (Precipitation flag and profiles) provide cloud microphysical information. Aerosol profiling is provided by CALIOP-CALIPSO and their optical properties are taken from D'Almeida et al. (1991) and WCP-55 (1983). The mixing ratios of methane, carbon dioxide and nitrous oxide are held uniform at 1.6, 360.0 and 0.28 ppmv respectively. Additional information on surface and zenith angles is taken from AN-ALBEDO, AMSR-AUX and MODIS-AUX products.

At each location, atmospheric profiles from CloudSat are available only at a certain times of the day, Hence, the shortwave heating rates are normalized by a factor (an example is shown below) that takes into account the diurnal variation of insolation. The normalization factor is computed as follows:

To calculate the flux density of solar radiation (Q) a combination of the inverse-square law and Lambert's cosine law is used.

$$Q = S_\mathrm{o}\frac{R_\mathrm{o}^2}{R_\mathrm{E}^2}\cos\Theta \text{ when } \cos\Theta > 0$$

$$Q = 0 \text{ when } \cos\Theta \leq 0 \tag{1}$$

Where S_o is the solar constant, R_o is the mean distance to the sun from earth while R_E is the actual distance between Earth and Sun. The Θ is the solar zenith angel and can be defined using the spherical law of cosines

$$\cos(\Theta) = \sin(\phi)\sin(\delta) + \cos(\phi)\cos(\delta)\cos(h) \tag{2}$$

where ϕ is the latitude, δ is the solar declination and h is the hour angle. To calculate the mean flux density of solar radiation for one day the average of one Q over one rotation is calculated. During one rotation h progresses from π to $-\pi$.

$$\overline{Q}^{\mathrm{day}} = -\frac{1}{2\pi}\int_{\pi}^{-\pi} Q\,\mathrm{d}h \tag{3}$$

ACPD
15, 5423–5459, 2015

Vertical structure of cloud radiative heating

E. Johansson et al.

Solving Eq. (3) will give

$$\overline{Q}^{\mathrm{day}} = \frac{S_\mathrm{o}}{\pi}\frac{R_\mathrm{o}^2}{R_\mathrm{E}^2}\left[h_\mathrm{o}\sin(\phi)\sin(\delta) + \cos(\phi)\cos(\delta)\sin(h_\mathrm{o})\right] \tag{4}$$

where h_o is the hour angle when Q becomes positive i.e. when $\Theta = \frac{1}{2}\pi$.

The normalization factor is then,

$$f = \frac{\overline{Q}^{\mathrm{day}}}{Q} \tag{5}$$

$$f = \frac{h_\mathrm{o}\sin(\phi)\sin(\delta) + \cos(\phi)\cos(\delta)\sin(h_\mathrm{o})}{\pi\cos\Theta} \tag{6}$$

Then for each cloud type studied here, the CRH is calculated as:

$$\mathrm{CRH} = ((f\cdot\mathrm{SWHR}_{\mathrm{cloudy}} + \mathrm{LWHR}_{\mathrm{cloudy}}) - (f\cdot\mathrm{SWHR}_{\mathrm{clear}} + \mathrm{LWHR}_{\mathrm{clear}}))\cdot\mathrm{CF} \tag{7}$$

where SWHR and LWHR are shortwave (normalized by the factor f mentioned above) and longwave heating rates respectively. CF is the absolute fraction of cloud type in question. By weighing with cloud fraction, we get the absolute contribution of that particular cloud type. For each height bin, CF is computed by dividing the number of cloudy pixels of a particular cloud type by the total number of pixels (cloudy and clear).

We used the 2B-FLXHR-LIDAR data from 2006 to 2010 and for May through October, since the focus of the study is on summer monsoon and pre- and post-monsoon periods. The study investigates high clouds (cirrus), deep convective clouds and the third type combining alto- and nimbostratus (referred to as stratiform clouds later). These cloud types are selected for the following reasons. (1) Collectively, their relative frequency of occurrence is from 65 to 85 % depending on location and month (refer Fig. 2). (2) These cloud types should have the largest impact on the UTLS region (Dessler and Sherwood, 2004; Gettelman et al., 2002; Rossow and Pearl, 2007), which is the main

Discussion Paper | Discussion Paper | Discussion Paper | Discussion Paper |

ACPD

15, 5423–5459, 2015

Vertical structure of cloud radiative heating

E. Johansson et al.

focus of the present study. We used collocated 2B-CLDCLASS-LIDAR product to obtain information on selected cloud types.

Figure 3 shows the study area and three zones selected for investigation of the vertical structure of CRH. The selection is based on previous studies of the description of cloud variability over the study area (Devasthale and Grassl, 2009; Devasthale and Fueglistaler, 2010) and the distribution of precipitation. The first zone (65–75° E, denoted Z1) covers western equatorial Indian Ocean and Arabian Sea, the parts of the subcontinent that experience the first monsoon showers and show largest variability in convective activity during active/break periods of monsoon. Z1 covers the southwestern coast of India that experiences very high amount of rainfall (Fig. 3b). The second zone (75–85° E, Z2) covers central and southern Indian regions, while the third zone (85–95° E, Z3) covers the Bay of Bengal, northeastern parts of India and the Tibetan Plateau. These regions are subjected to the most intense convection over the subcontinent, and also receive highest amount of rainfall during the monsoon season (Fig. 3b).

3 Results and discussions

3.1 Vertical distribution of clouds over the Indian subcontinent

This section presents information on the vertical distribution of cloud fraction, which is required to interpret the effect of CRH. To understand the implication of the CRH produced by different cloud types, an overview of the cloud liquid and ice water paths of different cloud types, and their net cloud radiative effect, is also provided.

The majority of clouds over the subcontinent are present between 5 and 16 km in height, thus most likely consisting of ice (Fig. 4). The vertical distribution of individual cloud types is shown in the Figs. S1 to S3. In May, all cloud types are prevalent around the equatorial Indian Ocean, but their progression towards continental India in response to the strengthening of the monsoonal circulation in subsequent months is also clearly visible. The highest and the most intense clouds are observed in Z3 over the Bay of Bengal and northeastern Indian regions. The vertical cloud fraction peaks during June and July over the majority of the continent. In August, the cloud fraction is still high over northern India. At the end of August and in September, cloud fraction decreases sharply as the monsoonal circulation weakens. The lowest cloud fraction is thus observed during September. In October, the intense band of cloudiness is shifted to lower latitudes, even south of the equator. The onset of the northeast monsoon causes increased cloudiness in October compared to September.

Although the intraseasonal migration of clouds during the summer monsoon has been studied before in more general terms (e.g. Devasthale and Grassl, 2009; Devasthale and Fueglistaler, 2010), the detailed vertical structure obtained from the data displayed in Fig. 4 provides additional insights. For example, the intraseasonal variability of clouds above the bottom of the tropical tropopause layer (TTL), here represented by the level of clear-sky zero radiative heating (LZRH) and shown as a white line in Fig. 4, provides an indication of the potential role of clouds in providing water vapor to the UTLS and also affecting other UTLS processes. The vertical cloud fraction above LZRH remains surprisingly very high from June through August and clouds clearly penetrate into the TTL. Figure 4 further reveals differences in cloudiness and cloud height over the Tibetan Plateau compared to the southern slopes of Himalayas and the Bay of Bengal. It is evident in Z2 and Z3, that include parts of the Tibetan Plateau (28–40° N), that the majority of clouds remain below LZRH in contrast to the Bay of Bengal and the southern slopes of Himalayas where they are prevalent well into the TTL.

Figure 5 shows the probability density functions (pdf) of liquid and ice water paths of the three cloud types selected for further analysis in the present study based on 2B-CWC-RVOD data set. High clouds by definition do not contain liquid water, while all three types contain ice. In the case of high clouds, the pdf of ice water path follows a sharp exponential distribution. For stratiform clouds, the pdf also follows similar distribution, but has lower value of rate parameter (thus making it broader). The pdfs of deep convective clouds follow gamma distribution. It is to be noted that CloudSat/CPR in itself cannot detect the thermodynamic phase of the hydrometeors. It relies on an-

ACPD
15, 5423–5459, 2015

cillary input from ECMWF (temperature profiles) and MODIS to partition total cloud condensate into ice and liquid fractions by linearly scaling them between −20 to 0 °C in the vertical. This introduces some uncertainty in the estimates of liquid and ice water paths (Devasthale and Thomas, 2012).

3.2 CRH during the monsoon

Figure 6 provides an overview of CRH separated into its daytime shortwave (SW) and longwave (LW) components and averaged over the core monsoon season (i.e. June through September). We observe noticeable differences in the CRH magnitude and spatial distribution in the three selected zones. For example, the vertical gradient in the SW heating steepens from Z1 to Z3 in the uppermost troposphere north of the equator. The seasonally averaged SW heating with values exceeding 0.25 $\mathrm{K\,day^{-1}}$ remains predominantly near the equatorial regions in Z1 and gradually extents towards northerly regions in Z2 and Z3. The SW heating follows to a large extent the vertical distribution of cloud fraction (cf. Fig. 4) with the highest values (of the order of 0.5 $\mathrm{K\,day^{-1}}$) found over Z3 at 15–20° N and 12–16 km altitude. In general, the SW heating takes place in the upper troposphere below the LZRH (except possibly over Z3 around 20° N). One noticeable exception is the Tibetan Plateau, where the heating takes place below 10 km and is of similar magnitude in Z2 and Z3. As a seasonal average, the upper troposphere predominantly experiences cloud radiative cooling in the LW component. The LW cooling mainly takes place in the upper troposphere, below the LZRH, and is highest in Z3, over the Bay of Bengal and the southern slopes of the Himalayas, mainly as a result of cooling from the tops of stratiform and convective clouds (cf. Supplement). Over the Tibetian Plateau, the high frequency of stratiform clouds gives rise to a cooling, in particular over Z2 and Z3. The effect of the melting layer at around 5 km is also visible in Fig. 6. The LW cooling pattern is in general patchier than the SW warming pattern, and in some parts of the troposphere clouds actually generate an overall LW heating during the monsoon period. The Figs. S4–S6 present individual contribution of high clouds, deep convection and combined alto- and nimbostratus clouds to the total SW and LW

ACPD
15, 5423–5459, 2015

heating rates separately. The observed patchiness in the LW component in the upper troposphere can be explained by opposing heating and cooling effects from different cloud categories at different levels. For example, the high cloud category, containing thin cirrus with low water content, generally warms the upper troposphere between 10 and 15 km. On the other hand, deep convective clouds and stratiform clouds, with higher water contents than cirrus, cool the atmosphere in the same layer.

The climatological cloud fraction (Fig. 4), cloud water path (Fig. 5) and CRH discussed above lead to a net cooling at the surface as shown in Fig. 7, when averaged over all cloud types and summer months (JJAS). The atmosphere is, on the other hand, warmed considerably due to cloud radiative effects. Cloud radiative effects from the Clouds and Earth's Radiant Energy System (CERES, EBAF-TOA and EBAF-Surface) sensor onboard NASA's Earth Observing Satellites for the summer months from 2006 through 2011 are presented in Fig. 7 (CERES data are used here to illustrate spatial patterns due to their better spatial sampling relative to CloudSat and CALIPSO). It is to be noted that both the surface cooling and atmospheric warming are strongest over those regions where the frequency of deep convective clouds and optically thick stratiform clouds is also high.

3.3 Monthly evolution of CRH

The radiative heating in the troposphere over the Indian subcontinent is mainly driven by water vapour and aerosols during pre-monsoon phases. Apart from local anthropogenic sources, transport of dust, sea-salt and other natural aerosols from the Indian Ocean and Arabian Peninsula contributes to the total aerosol load over the subcontinent once the direction of winds becomes westerly or southwesterly in May. The land–sea thermal contrast further draws in moisture over the land from the neighbouring seas and sets the stage for rainfall onset. Given the distinct monthly variability in cloud fraction from pre- to post monsoon, examining corresponding monthly variations of CRH provides interesting insights that can be directly evaluated in the global climate models. Although a majority of the total rainfall is produced by the convective cores, the

ACPD
15, 5423–5459, 2015

absolute fraction of these cores is usually very low. Other cloud types, such as outflow anvils produced during the life cycle of a typical convective system and stratus clouds, stay longer in the atmosphere, and thus could eventually have higher radiative impact over time. Therefore, we investigated the temporal evolution of the individual contribution of the different cloud types to CRH by taking into account their absolute spatial and vertical fraction.

Figure 8 shows the monthly evolution of total (LW + SW) CRH for deep convective clouds. Among the different cloud types studied here, the systematic monthly meridional progression of CRH is most clearly visible for these clouds. The convective cores warm nearly the entire troposphere, in some areas from 1 km to up to 14 km, but also cause strong net cooling at cloud top in the uppermost troposphere. In Z1, the convective contribution to CRH is limited to the equatorial region in May and it is not until August that the highest CRH over land (around 30° N) is observed when both the easterly branch of monsoonal circulation from the north-central India and the westerly branch from the Arabian Sea provide conducive conditions for deep convection. For all regions, the cooling due to convective cores extends above the base of the TTL, in particular over Z2 and Z3 from June to August between 10 and 20° N. This result is in agreement with previous observations by Zipser et al. (2006), who used data from the Tropical Rainfall Measurement Mission (TRMM) to show that the most intense thunderstorms (essentially caused by these convective cores) in the world occur over this region. Previous studies also report the Bay of Bengal and southern foothills of Himalayas supporting environments conducive for the penetrative convection during summer monsoon (James et al., 2008; Devasthale and Fueglistaler, 2010). Figure 8 clearly supports these previous results.

The monthly total CRH due alto- and nimbostratus clouds is shown in Fig. 9. In June–August, very distinct warming (values exceeding 0.2 $\mathrm{K\,day^{-1}}$ in average after normalizing with cloud fraction) in the middle troposphere (4–9 km) and equally strong cooling in the upper troposphere (between 9 km and LZRH) are observed in all regions. In August, the cooling at the top is partly offset by warming, mainly due to high vertical

Discussion Paper | Discussion Paper | Discussion Paper | Discussion Paper |

ACPD

15, 5423–5459, 2015

Vertical structure of cloud radiative heating

E. Johansson et al.

variability of these clouds in this particular month caused by the late advection of the eastern branch of the monsoon in the upper troposphere while the western branch triggering relatively shallow convection. The CRH due to these clouds is either very weak or nearly absent in September.

High clouds, either of convective origin or the result of the large-scale vertical ascent, warm the base and interior of the TTL (Fig. 10). Irrespective of their origin, it is clear that high thin clouds play a key role in assisting the gradual and large-scale vertical transport of upper tropospheric air into the stratosphere as these clouds provide the highest heating rates above the TTL (Fig. 10). Over the Arabian Sea (Fig. 10, Z1), the maximum heating of the TTL due to these clouds occurs in June, while over land, the peak is in August. It is worth noting that this coincides with the highest heating by convective clouds, also observed during the month of August, thus indicating a greater control by convective processes compared to large-scale ascent in this particular month and latitude band.

3.4 CRH in the TTL

In order to gain insights into the net effect of deep convective clouds and cirrus on the TTL, the probability density functions of CRH for those data bins that are located above the LZRH during summer monsoon months (May–August) are presented in Fig. 11. All data north of the equator from three zones are analysed to improve statistical sampling. Deep convection causes a net cooling of the TTL from May through July, but the PDFs become broader as the monsoon progresses. The largest average cooling rate is observed during July ($-4.20\,\mathrm{K\,day^{-1}}$) but the same month also displays the highest SD ($3.12\,\mathrm{K\,day^{-1}}$), meaning that there are more extreme events in general and that some events actually warm the TTL. The impact of deep convective clouds on the TTL is strongly reduced in August. Previous studies (Devasthale and Grassl, 2009; Devasthale and Fueglistaler, 2010), based on optical imagers, also argued that the most intense and penetrative convective events occur during early phases of the mon-

ACPD
15, 5423–5459, 2015

soon. By August, the surface temperatures over the subcontinent are relatively low and favourable conditions for penetrative convection no longer persist.

The net effect of high clouds on the TTL is a warming during all active months of the monsoon. The mean warming effect is lowest in July when convection is most active. As evident in the PDF, this is because some of the high clouds are cooling during this month. Considering that the deep convection exhibits the strongest cooling in this month, we believe that the cooling effect of high clouds may be due to remnants of deep convection (such as tops of relatively thick anvil cirrus, cirrostratus, etc.) emitting at much colder temperature and/or having higher water contents than thin or semitransparent cirrus would in other cases.

3.5 The role of active and break periods

Intra-seasonal oscillations are one of the intrinsic characteristics of Indian summer monsoon rainfall and occur as active and break conditions with no fixed periodicity. During active periods, high precipitation amounts are experienced over much of the subcontinent. These phases are usually followed by periods of reduced rainfall, called break periods. The mechanism behind these oscillations remains a topic of active research, however it is beyond doubt that they play an important role in modulating the seasonal mean rainfall distribution and amount over the subcontinent. For example, Goswami and Ajaya Mohan (2001) demonstrated that stronger than normal summer monsoon rainfall is associated with a higher frequency of active conditions. Enhanced cyclonic flow and convection is often observed during active periods. Enhanced upward motion in the northern position of the ITCZ is also observed during active conditions. This intraseasonal variability in rainfall (and convective clouds and associated anvils, cirrus etc.) has direct relevance for the distribution of heat and moisture within a given monsoon season.

Over the subcontinent itself, large variations in the spatial distribution of convection (and associated clouds) occur during active and break periods. Using 25 years of AVHRR-based cloud climatology, Devasthale and Grassl (2009) showed that convec-

ACPD
15, 5423–5459, 2015

tion extends far northwards and covers nearly the entire northern India during active phases. Especially the convective activity over the Arabian Sea is enhanced during this period, while during break periods, convection is restricted to the Bay of Bengal, southern slopes of Himalayas and the north-eastern parts of the continental India. Using the same data set, Devasthale and Fueglistaler (2010) further investigated very deep and penetrating convection (into the TTL). They showed that the penetrating convection is substantially suppressed in the western parts of the subcontinent during break periods and argued that active periods, although less frequent, could have large influence on the composition of the TTL.

Here we add a new dimension to these earlier studies by investigating the radiative effects of deep convection and high clouds during active/break periods in the UTLS region. The definition of these periods follows Rajeevan et al. (2010). Figure 12 shows the PDFs of instantaneous CRH for those cloudy bins of CloudSat-CALIPSO that are located above 10 km and LZRH, respectively, observed north of the equator. Deep convection has mean cooling effect in absolute terms above LZRH during both active ($-1.23\,\mathrm{K\,day^{-1}}$) and break periods ($-0.36\,\mathrm{K\,day^{-1}}$). However, the active conditions show much wider PDFs of CRH, in particular on the warming side of the distribution, suggesting that deep convection could affect the TTL very differently during active periods, compared to break periods. If the upper troposphere is also included in the analysis (i.e. cloud tops > 10 km), then deep convection produces an even stronger warming during active conditions compared to breaks (and the PDF is still broader). This is due to the fact that convection is more widespread in general and penetrates deeper during active periods.

For high clouds, the mean warming effect above LZRH is more than twice as large during active periods, compared to break periods. After including high clouds with tops located higher than 10 km, the warming during active conditions is still more than that observed during break periods, albeit not as strong in magnitude.

ACPD
15, 5423–5459, 2015

3.6 Cloud radiative effects at the surface and in the atmosphere

Considering the ubiquity of clouds during monsoon months and their radiative heating/cooling potential in the atmosphere discussed in Sects. 3.1–3.5, it can be argued that cloud radiative effect (CRE), in addition to latent heating, could be a large contributor to the total diabatic heating and also to the total energy budget in the atmosphere and at the surface. The tangible way to evaluate the resulting cloud impact on the surface is to investigate net CRE (expressed in terms of $\mathrm{W\,m^{-2}}$). This metric is commonly used in energy budget studies and to evaluate climate models. In our case, investigating CREs at surface provides insights into the role of different cloud types in acting as a potential "regulator" of monsoonal circulation by modulating spatial and vertical thermal contrast.

Table 1 summarizes mean daytime CRE values and their SD for different cloud types over selected zones, both at the surface and in the atmosphere. It can be seen that at surface, the net CRE remains strongly negative in all three zones for all cloud types. For stratiform and deep convective clouds, CREs vary considerably in the three zones, while the net impact of high clouds is similar. The deep convective clouds have a strong negative forcing at the surface which increases from Z1 to Z3. This is in agreement with the increasing fraction of these clouds from Z1 to Z3 and with increasing cloud condensate. Furthermore, it agrees with the spatial pattern of net CRE at surface obtained from the CERES data, wherein strongest cooling is observed in the regions with higher fraction of deep convective clouds. The stratiform clouds also cause strong surface cooling, albeit not as strong as deep convection. High values of SD in all cases indicate that a large variability exists in the net impact of these cloud types on the surface, depending on their physical and microphysical properties. Table 1 further shows that the net CRE leads to substantial atmospheric warming that is highest in the case of deep convective clouds and follows the same increasing tendency from Z1 to Z3.

Table 2 further shows the daytime CRE during active and break conditions of monsoon averaged over the all three zones northwards of the Equator. It is interesting

ACPD
15, 5423–5459, 2015

to note the relative differences in the cooling effect of stratiform and deep convective clouds at the surface. While the cooling by deep convective clouds is stronger during active phases, it is relatively weaker in the case of stratiform clouds. This is mainly because of the different frequency of occurrence of these cloud types during active and break periods of monsoon. As mentioned before, convective activity is suppressed during break periods (especially along the western coast of India), while the presence of less vigorous clouds such as nimbostratus and altostratus is enhanced (Devasthale and Grassl, 2009). Thus the CRE of deep convection is reduced while that of stratiform clouds is increased during break periods. It is to be noted that occasionally some of the most intense thunderstorms occur during break periods due to the build up of moist energy and very warm surface temperatures due to increased insolation at surface due to the lack of clouds, especially along the southern foothills of Himalayas (Vellore et al., 2014). Although the instantaneous CRE of such events could be very high, due to their very low frequency, the net CRE is also very low when averaged over the month and the wider area.

4 Conclusions

Clouds are intrinsically tied to the atmospheric circulation and radiation budget. The focus of the present study has been on understanding the influence of clouds on the different parts of the atmosphere and the surface, via their radiative effects during the Indian summer monsoon. Such quantification may provide insights into interactions of clouds with monsoonal circulation.

The vertical structure of CRH follows the northward migration and withdrawal of the monsoon from May to October over the subcontinent. It was found that the alto- and nimbostratus clouds intensely warm the middle troposphere and equally strongly cool the upper troposphere. Even after weighing by their vertical fraction, their warming/cooling consistently exceeds $\pm 0.2\,\mathrm{K\,day^{-1}}$ in monthly mean composites throughout the middle and upper troposphere, respectively, and their largest impact is observed

Discussion Paper | Discussion Paper | Discussion Paper | Discussion Paper |
ACPD
15, 5423–5459, 2015
Vertical structure of cloud radiative heating
E. Johansson et al.

in June, July and August. In contrast, high clouds representing thin cirrus, cirrostratus, cirrocumulus etc. and dominating the total cloud fraction, cause a considerable warming in the upper troposphere, with values between 0.1–0.2 K day^{-1} around the base of the TTL. Their largest impact is seen during the early phases of monsoon (May–July). Deep convective towers warm nearly the entire troposphere, but have a net cooling effect at the base of the TTL. While individual convective cores may produce extreme heating, their occurrence is very low and thus the net effect is smaller than that of alto- and nimbostratus and high clouds.

The net radiative impact of high clouds and deep convection on the TTL was also investigated revealing that during the monsoon, deep convection generally causes strong instantaneous cooling inside the TTL and the intensity of cooling increases with the monthly progress of monsoon until July when the strongest cooling is observed (mean -4.2 K day^{-1}). However, the PDFs of CRH also become broader as the monsoon progresses and during July such that some clouds classified as deep convection radiatively heat the TTL. High clouds, on the other hand, generally lead to net warming effect. Deep convection has mean cooling effect in absolute terms above LZRH during both active (-1.23 K day^{-1}) and break periods (-0.36 K day^{-1}). However, the active conditions show much wider PDFs of CRH suggesting that convective clouds not always cool the TTL. In case of high clouds, the mean net warming effect above LZRH is more than double in magnitude during active conditions compared to break periods. The present study also underscores the importance of Bay of Bengal and the foothills of Himalayas in supporting the deep and penetrative convection and its remnants.

Finally, it is shown that the stratiform clouds and deep convection significantly cool the surface with a net radiative effect around -100 and -400 W m^{-2}, respectively. The high clouds also have a cooling radiative effect at the surface, albeit of small magnitude compared to other cloud types. The atmospheric warming purely due to radiative effects of clouds is also very high, in the order of 40 and 150 W m^{-2} in case of stratifrom and deep convective clouds respectively. The magnitude of radiative effects of convective clouds increases from the western to eastern parts of the subcontinent, while the importance of stratiform clouds is higher in the western parts. While the deep convection produces strong cooling at the surface during active periods of monsoon, the importance of stratiform clouds on the other hand increases during break periods.

The contrasting CREs in the atmosphere and at surface, and also during active and break conditions, should have direct implications for monsoonal circulation. It is evident that clouds reduce the land surface temperatures over the subcontinent, thus reducing the land–sea thermal contrast that initially sets up the favourable conditions for the onset of monsoon during pre-monsoon months. Although this thermal contrast is reduced by clouds, the net radiative warming of the atmosphere by clouds in concert with their latent heating likely sustains the thermal gradient in the atmosphere (Webster et al., 1998). Although the large-scale dynamics (e.g. position and movement of monsoon trough) probably has the first order impact on regulating the intraseasonal oscillations (and hence active and break periods), the differences in the frequency of occurrence of different cloud types represented an important feedback in conditioning these periods via their radiative effects. For example, the strong surface cooling observed during active periods could help suppress the convection in the following days, thus leading to break in monsoon conditions. The studies involving climate models will further be needed to shed light on these aspects.

The Supplement related to this article is available online at doi:10.5194/acpd-15-5423-2015-supplement.

References

D'Almeida, G. A., Koepke, P., and Shettle, E. P.: Atmospheric Aerosols: Global Climatology and Radiative Characteristics, A. Deepak, 561 pp., University of California, USA, ISBN-13: 978-0937194225, 1991.

Dessler, A. E. and Sherwood, S. C.: Effect of convection on the summertime extratropical lower stratosphere, J. Geophys. Res., 109, D23301, doi:10.1029/2004JD005209, 2004.

Devasthale, A. and Fueglistaler, S.: A climatological perspective of deep convection penetrating the TTL during the Indian summer monsoon from the AVHRR and MODIS instruments, Atmos. Chem. Phys., 10, 4573–4582, doi:10.5194/acp-10-4573-2010, 2010.

Devasthale, A. and Grassl, H.: A daytime climatological distribution of high opaque ice cloud classes over the Indian summer monsoon region observed from 25-year AVHRR data, Atmos. Chem. Phys., 9, 4185–4196, doi:10.5194/acp-9-4185-2009, 2009.

Devasthale, A. and Thomas, M. A.: Sensitivity of cloud liquid water content estimates to the temperature-dependent thermodynamic phase: a global study using CloudSat data, J. Climate, 25, 7297–7307, doi:10.1175/JCLI-D-11-00521.1, 2012.

Feldman, D. R., L'Ecuyer, T. S., Liou, K. N., and Yung, Y. L.: Remote sensing of tropical tropopause layer radiation balance using A-Train measurements, J. Geophys. Res., 113, D21113, doi:10.1029/2007JD009041, 2008.

Fueglistaler, S. and Fu, Q.: Impact of clouds on radiative heating rates in the tropical lower stratosphere, J. Geophys. Res., 111, D23202, doi:10.1029/2006JD007273, 2006.

Fueglistaler, S., Dessler, A. E., Dunkerton, T. J., Folkins, I., Fu, Q., and Mote, P. W.: Tropical tropopause layer, Rev. Geophys., 47, RG1004, doi:10.1029/2008RG000267, 2009a.

Fueglistaler, S., Legras, B., Beljaars, A., Morcrette, J.-J., Simmons, A., Tompkins, A. M., and Uppala, S.: The diabatic heat budget of the upper troposphere and lower/mid stratosphere in ECMWF reanalyses, Q. J. Roy. Meteor. Soc., 135, 21–37, doi:10.1002/qj.361, 2009b.

Gettelman, A., Salby, M. L., and Sassi, F.: Distribution and influence of convection in the tropical tropopause region, J. Geophys. Res., 107, 4080, doi:10.1029/2001JD001048, 2002.

Gettelman, A., Kinnison, D. E., Dunkerton, T. J., and Brasseur, G. P.: The impact of monsoon circulations on the upper troposphere and lower stratosphere, J. Geophys. Res., 109, D22101, doi:10.1029/2004JD004878, 2004.

Goswami, B. N. and Ajaya Mohan, R. S.: Intraseasonal oscillations and interannual variability of the Indian summer monsoon, J. Climate, 14, 1180–1198, 2001.

Haynes, J. M., Vonder Haar, T. H., L'Ecuyer, T., and Henderson, D.: Radiative heating characteristics of Earth's cloudy atmosphere from vertically resolved active sensors, Geophys. Res. Lett., 40, 624–630, doi:10.1002/grl.50145, 2013.

Henderson, D. S., L'Ecuyer, T., Stephens, G., Partain, P., and Sekiguchi, M.: A multi-sensor perspective on the radiative impacts of clouds and aerosols, J. Appl. Meteorol. Clim., 52, 852–870, 2013.

ACPD

15, 5423–5459, 2015

Vertical structure of cloud radiative heating

E. Johansson et al.

James, R., Bonazzola, M., Legras, B., Surbled, K., and Fueglistaler, S.: Water vapor transport and dehydration above the convective outflow during Asian monsoon, Geophys. Res. Lett., 35, L20810, doi:10.1029/2008GL035441, 2008.

L'Ecuyer, T. S. and Jiang, J.: Touring the atmosphere aboard the A-Train, Phys. Today, 63, 36–41, 2010.

L'Ecuyer, T. S. and McGarragh, G.: A ten year climatology of atmospheric radiative heating and its vertical structure from TRMM observations, J. Climate, 23, 519–541, 2010.

L'Ecuyer, T. S., Wood, N., Haladay, T., and Stephens, G. L.: The impact of clouds on atmospheric heating based on the R04 CloudSat fluxes and heating rate detest, J. Geophys. Res., 113, D00A15, doi:10.1029/2008JD009951, 2008.

Ling, J. and Zhang, C.: Diabatic heating profiles in recent global reanalyses, J. Climate, 26, 3307–3325, doi:10.1175/JCLI-D-12-00384.1, 2013.

Luo, Z. and Rossow, W. B.: Characterizing tropical cirrus lifecycle, evolution and interaction with upper tropospheric water vapor using Lagrangian trajectory analysis of satellite observations, J. Climate, 17, 4541–4563, 2004.

Mace, G. G., Zhang, Q., Vaughan, M., Marchand, R., Stephens, G., Trepte, C., and Winker, D.: A description of hydrometeor layer occurrence statistics derived from the first year of merged Cloudsat and CALIPSO data, J. Geophys. Res., 114, D00A26, doi:10.1029/2007JD009755, 2008.

Mcfarlane, S. A., Mather, J. H., and Ackerman, T. P.: Analysis of tropical radiative heating profiles: a comparison of models and observations, J. Geophys. Res., 112, D14218, doi:10.1029/2006JD008290, 2007.

Park, M., Randel, W. J., Emmons, L. K., Bernath, P. F., Walker, K. A., and Boone, C. D.: Chemical isolation in the Asian monsoon anticyclone observed in Atmospheric Chemistry Experiment (ACE-FTS) data, Atmos. Chem. Phys., 8, 757–764, doi:10.5194/acp-8-757-2008, 2008.

Rajeevan, M., Gadgil, S., and Bhate, J.: Active and break spells of the Indian summer monsoon, J. Earth Syst. Sci., 119, 229–247, 2010.

Randel, W. J. and Park, M.: Deep convective influence on the Asian summer monsoon anticyclone and associated tracer variability observed with Atmospheric Infrared Sounder (AIRS), J. Geophys. Res., 111, D12314, doi:10.1029/2005JD006490, 2006.

Rossow, W. B. and Pearl, C.: 22-year survey of tropical convection penetrating into the lower stratosphere, Geophys. Res. Lett., 34, L04803, doi:10.1029/2006GL028635, 2007.

ACPD
15, 5423–5459, 2015

Vertical structure of cloud radiative heating

E. Johansson et al.

Sherwood, S. C., Bony, S., and Dufresne, J.-L.: Spread in model climate sensitivity traced to atmospheric convective mixing, Nature, 505, 37–42, 2014.

Stubenrauch, C. J., Rossow, W. B., Kinne, S., Ackerman, S., Cesana, G., Chepfer, H., Di Girolamo, L., Getzewich, B., Guignard, A., Heidinger, A., Maddux, B., Menzel, P., Minnis, P., Pearl, C., Platnick, S., Poulsen, C., Riedi, J., Sun-Mack, S., Walther, A., Winker, D., Zeng, S., Zhao, G.: Assessment of global cloud datasets from satellites: project and database initiated by the GEWEX Radiation Panel, B. Am. Meteorol. Soc., 1031–1049, doi:10.1175/BAMS-D-12-00117, 2012.

Tzella, A. and Legras, B.: A Lagrangian view of convective sources for transport of air across the Tropical Tropopause Layer: distribution, times and the radiative influence of clouds, Atmos. Chem. Phys., 11, 12517–12534, doi:10.5194/acp-11-12517-2011, 2011.

Vellore, R., Krishnan, R., Choudhury, A., Pendharkar, J., and Sabin, T.: On anomalous precipitation enhancement over the foothills of the Himalayas during break monsoons, Clim. Dynam., 43, 2009–2031, doi:10.1007/s00382-013-2024-1, 2014.

Wang, C., Kim, D., Ekman, A. M. L., Barth, M. C., and Rasch, P. J.: Impact of anthropogenic aerosols on Indian summer monsoon, Geophys. Res. Lett., 36, L21704, doi:10.1029/2009GL040114, 2009.

Webster, P. J., Magana, V. O., Palmer, T. N., Shukla, J., Tomas, R. A., Yanai, M., and Yasunari, T.: Monsoons: processes, predictability, and the prospects for prediction, J. Geophys. Res., 103, 14451–14510, 1998.

WCP-55: Report of the expert meeting on aerosols and their climate effects, World Meteorological Organization, Geneva, 107 pp., 1983.

Wright, J. S. and Fueglistaler, S.: Large differences in reanalyses of diabatic heating in the tropical upper troposphere and lower stratosphere, Atmos. Chem. Phys., 13, 9565–9576, doi:10.5194/acp-13-9565-2013, 2013.

Yang, Q., Fu, Q., and Hu, Y.: Radiative impacts of clouds in the tropical tropopause layer, J. Geophys. Res., 115, D00H12, doi:10.1029/2009JD012393, 2010.

Zipser, E. J., Cecil, D., Liu, C., Nesbitt, S., and Yorty, D.: Where are the most intense thunderstorms on earth?, B. Am. Meteorol. Soc., 87, 1057–1071, 2006.

ACPD
15, 5423–5459, 2015

Table 1. Area averaged (northwards of the Equator) daytime cloud radiative effect (CRE) and its SD (in brackets) of three selected cloud types. The months of JJAS are selected for analysis. All values are in $W\,m^{-2}$.

	High clouds	Stratiform	Deep convection
Atmosphere			
Z1	39 (40)	44 (45)	101 (18)
Z2	45 (46)	45 (43)	132 (25)
Z3	49 (49)	48 (47)	152 (32)
Surface			
Z1	−10 (36)	−133 (168)	−391 (157)
Z2	−13 (55)	−93 (162)	−410 (157)
Z3	−11 (53)	−114 (181)	−536 (144)

ACPD
15, 5423–5459, 2015

ACPD
15, 5423–5459, 2015

Vertical structure of cloud radiative heating

E. Johansson et al.

Table 2. Daytime cloud radiative effect (CRE) and its SD (in brackets) of three selected cloud types averaged over all three zones northwards of the Equator. The months of JJAS are selected for analysis. All values are in $W\,m^{-2}$.

	High clouds	Stratiform	Deep convection
Atmosphere			
Active	54 (49)	79 (57)	172 (38)
Break	43 (47)	108 (58)	178 (33)
Surface			
Active	−29 (51)	−155 (163)	−508 (164)
Break	−25 (47)	−180 (179)	−454 (135)

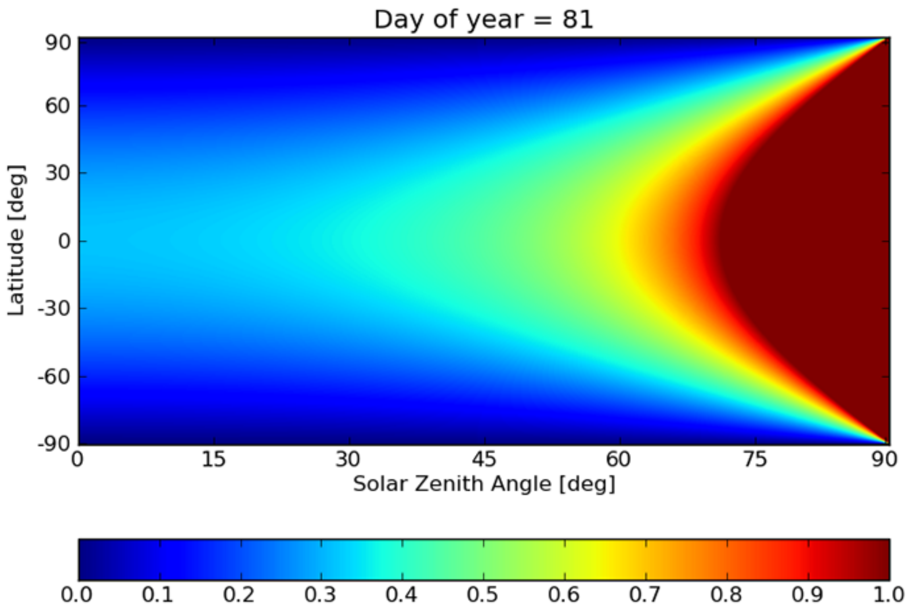

Figure 1. An example of normalization factor for the day 81 of a year as a function of latitude and solar zenith angle.

ACPD
15, 5423–5459, 2015

Vertical structure of cloud radiative heating

E. Johansson et al.

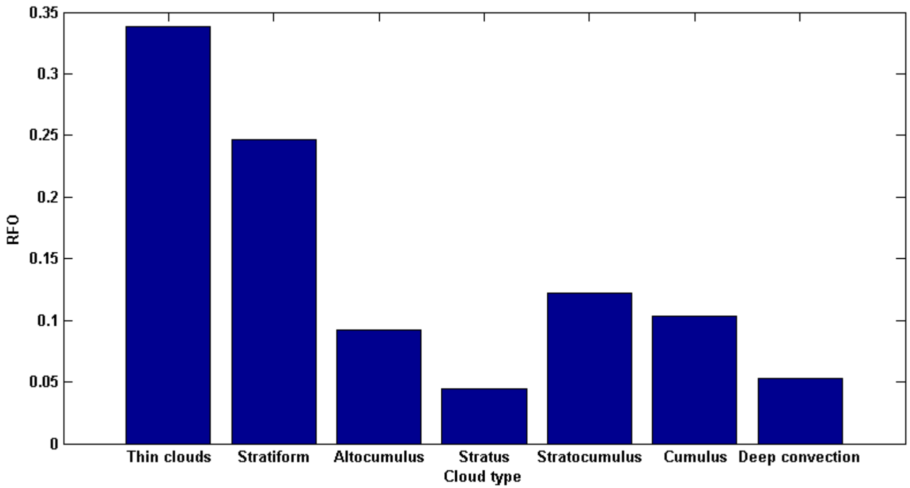

Figure 2. The relative frequency of occurrence (RFO) of different cloud types over the Indian subcontinent based on 2B-CLDCLASS-LIDAR product for the 2006–2010 period.

ACPD
15, 5423–5459, 2015

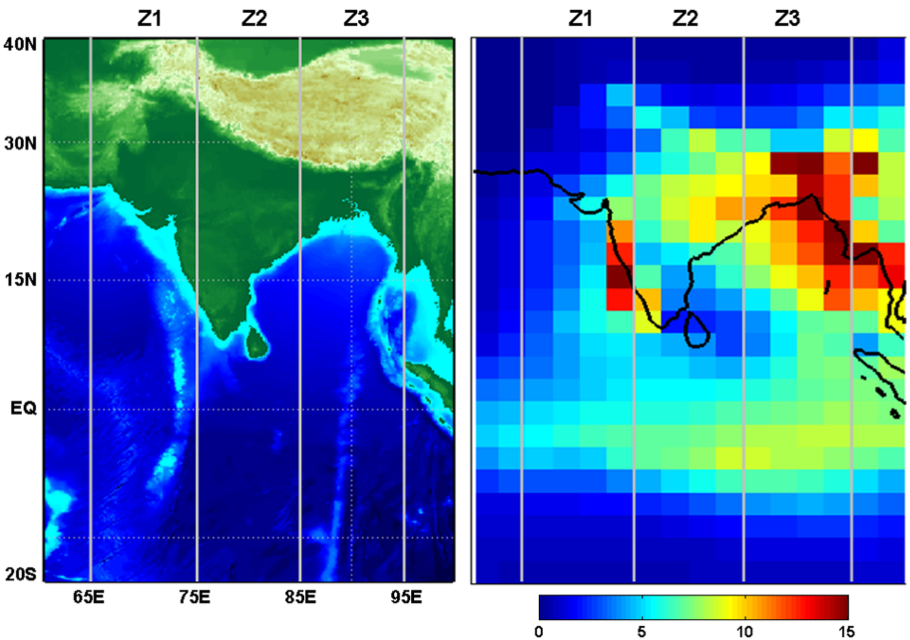

Figure 3. The study area and three selected zones (left panel) and climatological distribution of rainfall (mm day^{-1}, right panel) for summer monsoon (JJAS) obtained from the Global Precipitation Climatology Project Version 2.2 monthly data (G. J. Huffman, D. T. Bolvin, R. F. Adler, 2012, last updated 2012: GPCP Version 2.2 Satellite-Gauge Combined Precipitation Data Set. WDCA, NCDC, Asheville, NC. Data set accessed Sept 2014, at http://precip.gsfc.nasa.gov/gpcp_v2.2_data.html).

ACPD
15, 5423–5459, 2015

Vertical structure of cloud radiative heating

E. Johansson et al.

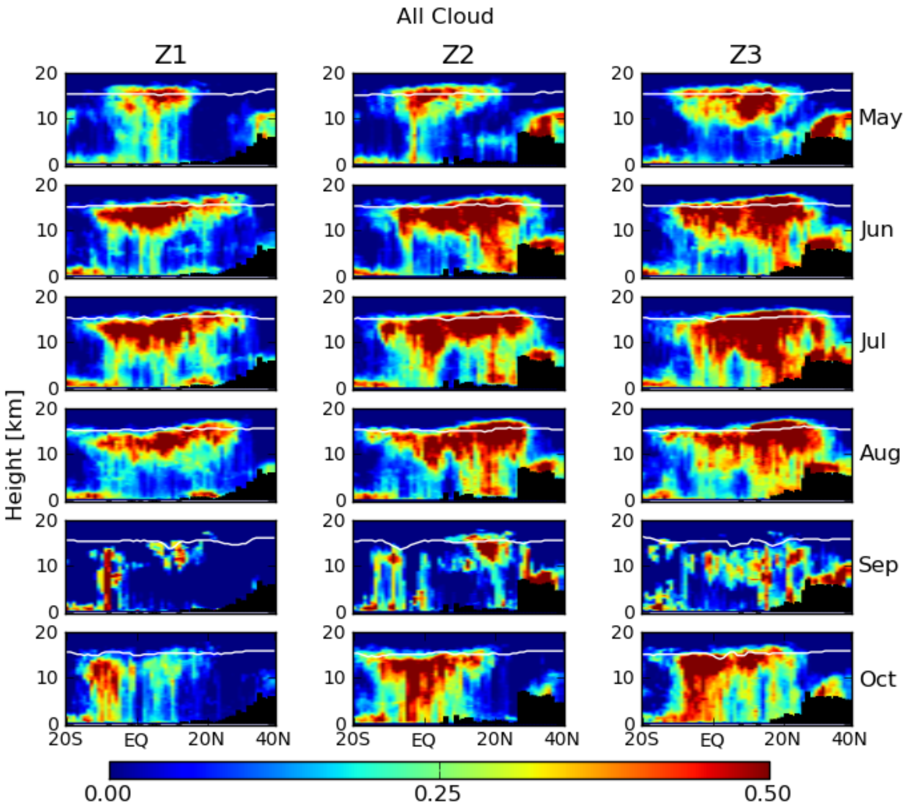

Figure 4. The vertical cloud fraction over the selected three zones (cf. Fig. 3) as a function of month. The white line represents the level of net clear-sky zero radiative heating as proxy for the base of the TTL.

ACPD
15, 5423–5459, 2015

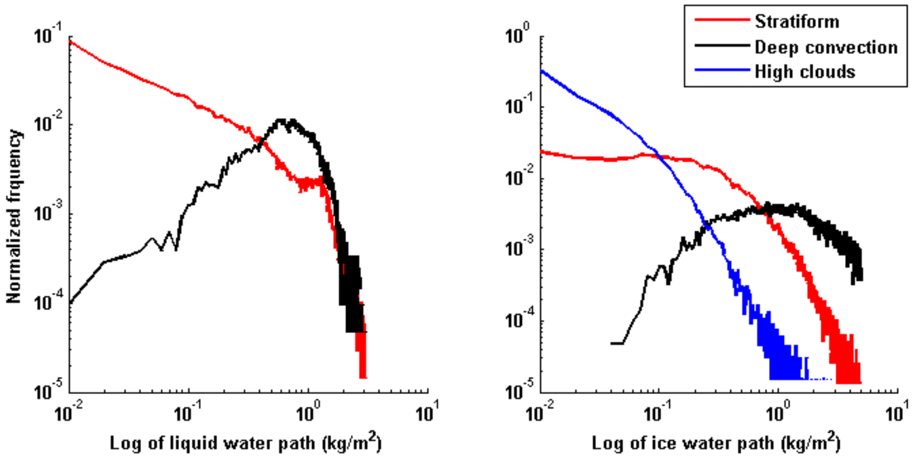

Figure 5. Probability density functions of liquid and ice water paths for the selected cloud types and for the summer monsoon months (JJAS) based on CloudSat's 2B-CWC-RVOD and 2B-CLDCLASS-LIDAR products.

ACPD
15, 5423–5459, 2015

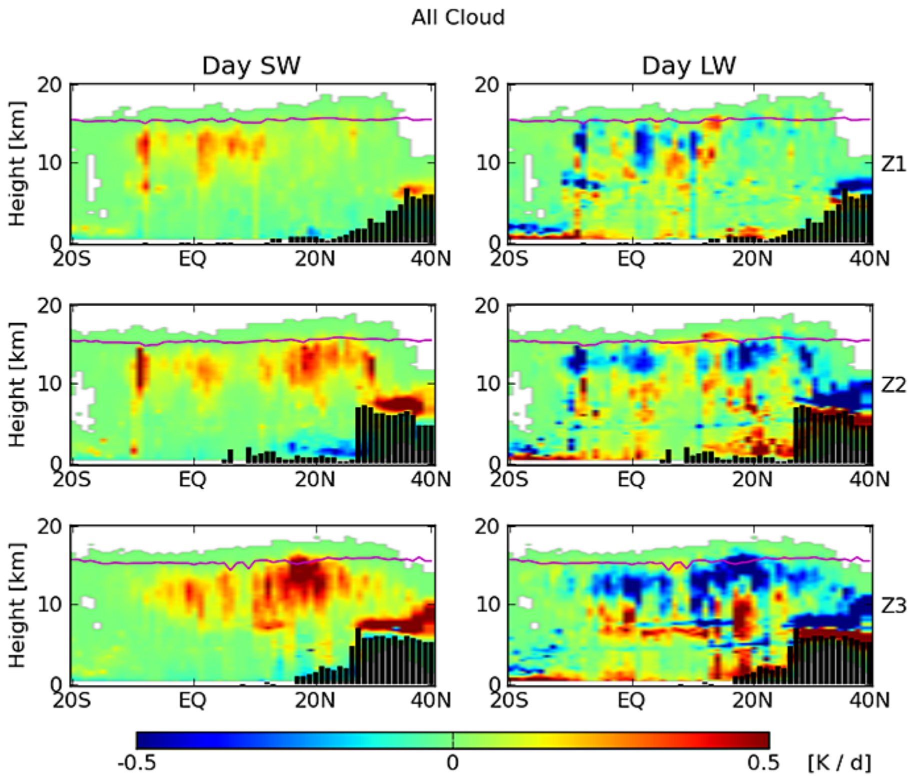

Figure 6. The vertical structure of CRH partitioned into its SW and LW components. All cloud types are included in the analysis and the data from 2006–2010 for the months June–September are used. The magenta coloured lines show the level of zero net clear-sky radiative heating (LZRH).

Discussion Paper | Discussion Paper | Discussion Paper | Discussion Paper |

Title Page
Abstract Introduction
Conclusions References
Tables Figures
◀| |▶
◀ ▶
Back Close
Full Screen / Esc
Printer-friendly Version
Interactive Discussion

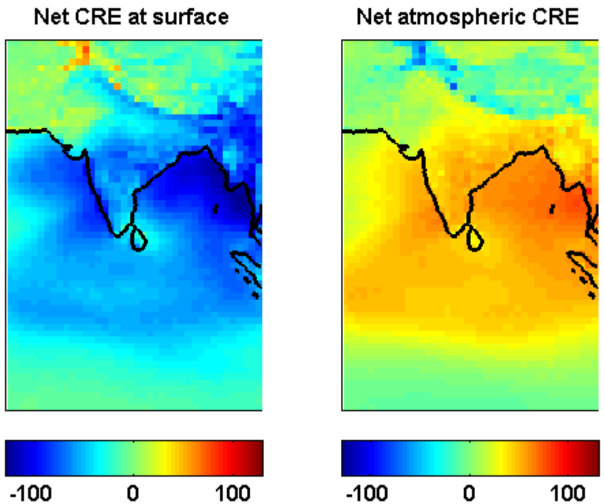

Figure 7. The net cloud radiative effect (in $W\,m^{-2}$) at surface and in the atmosphere based on CERES data averaged over the summer monsoon months (JJAS).

ACPD
15, 5423–5459, 2015

Vertical structure of cloud radiative heating

E. Johansson et al.

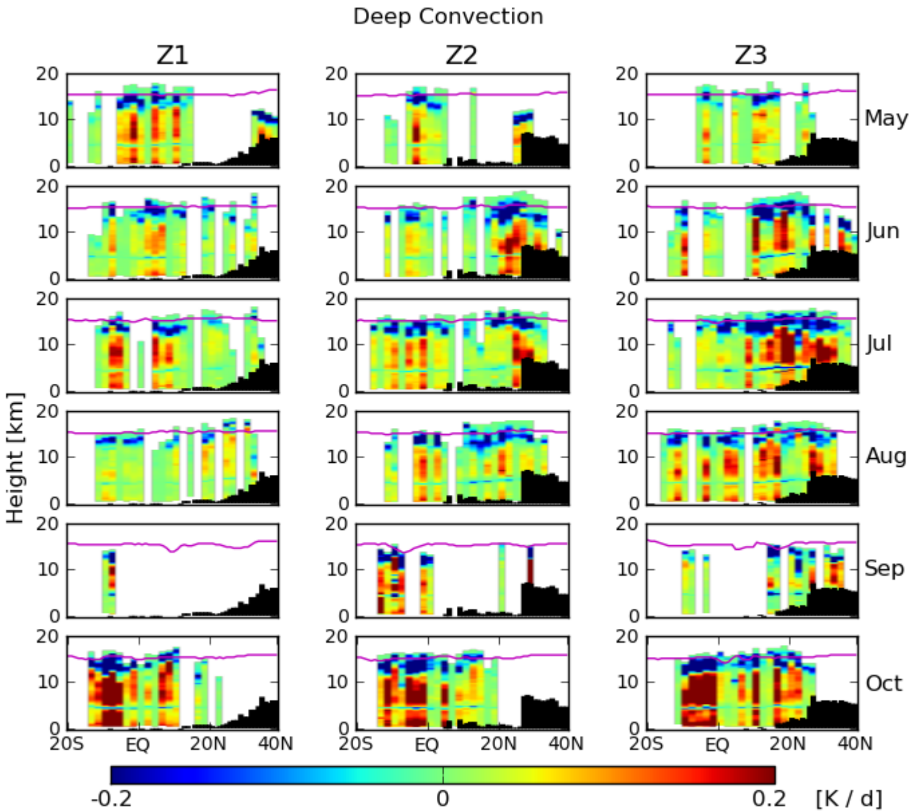

Figure 8. The monthly evolution of CRH due to deep convective clouds. The magenta coloured lines show the level of zero net clear-sky radiative heating (LZRH).

ACPD
15, 5423–5459, 2015

Vertical structure of cloud radiative heating

E. Johansson et al.

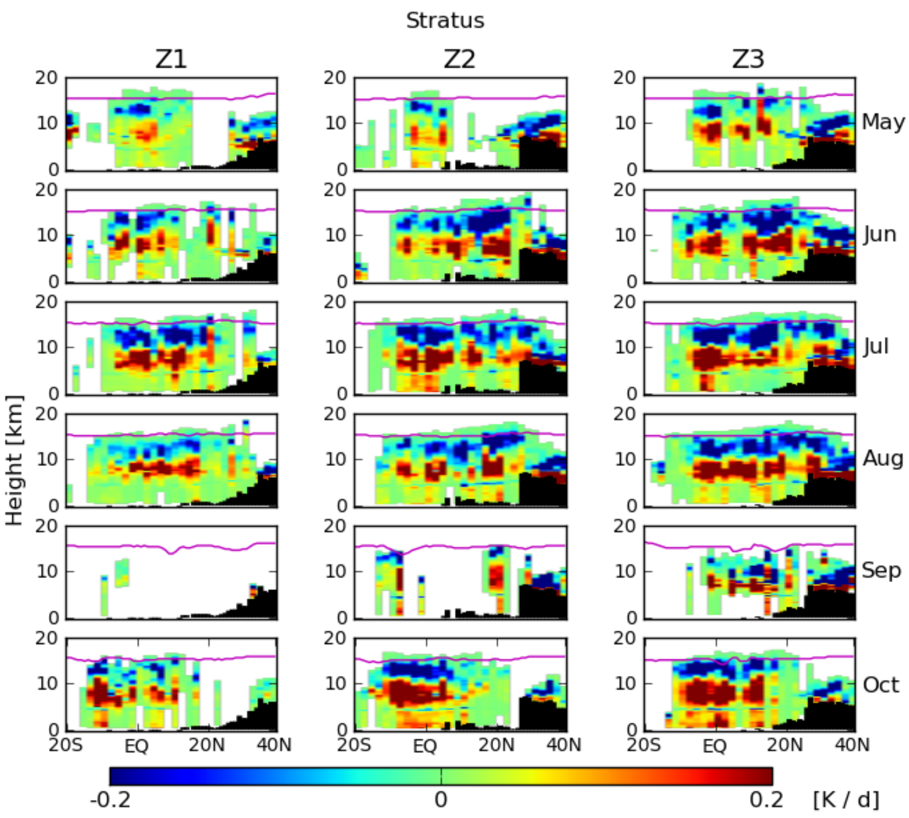

Figure 9. The monthly evolution of CRH due to alto- and nimbostratus clouds.

ACPD
15, 5423–5459, 2015

Vertical structure of cloud radiative heating

E. Johansson et al.

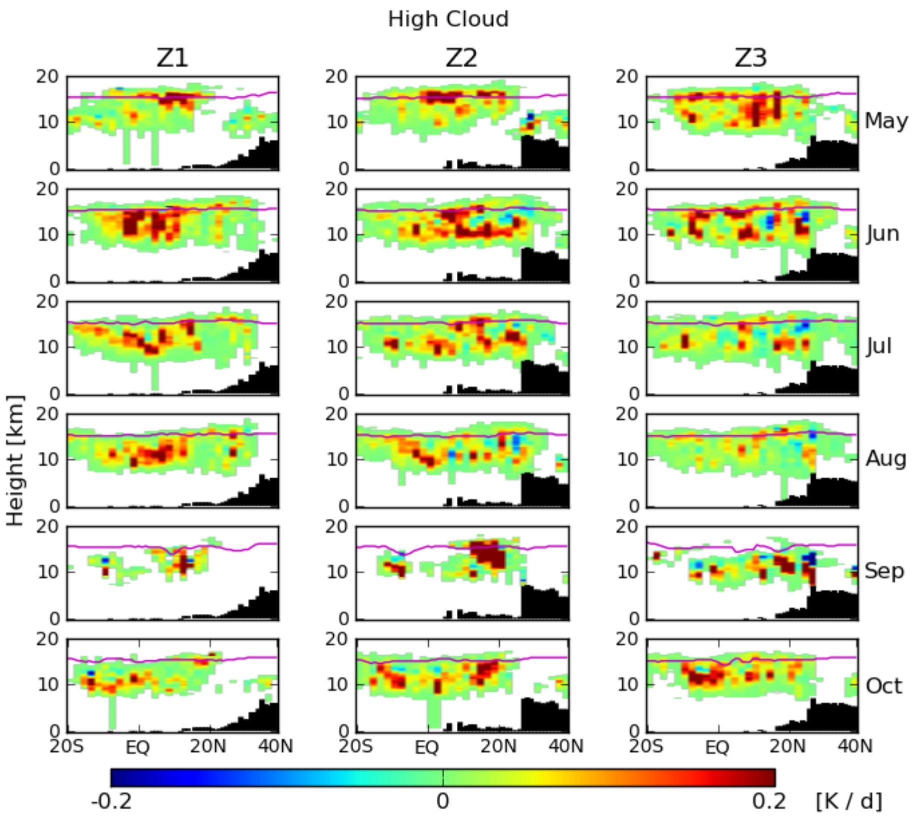

Figure 10. The monthly evolution of CRH due to high clouds.

ACPD
15, 5423–5459, 2015

Vertical structure of cloud radiative heating

E. Johansson et al.

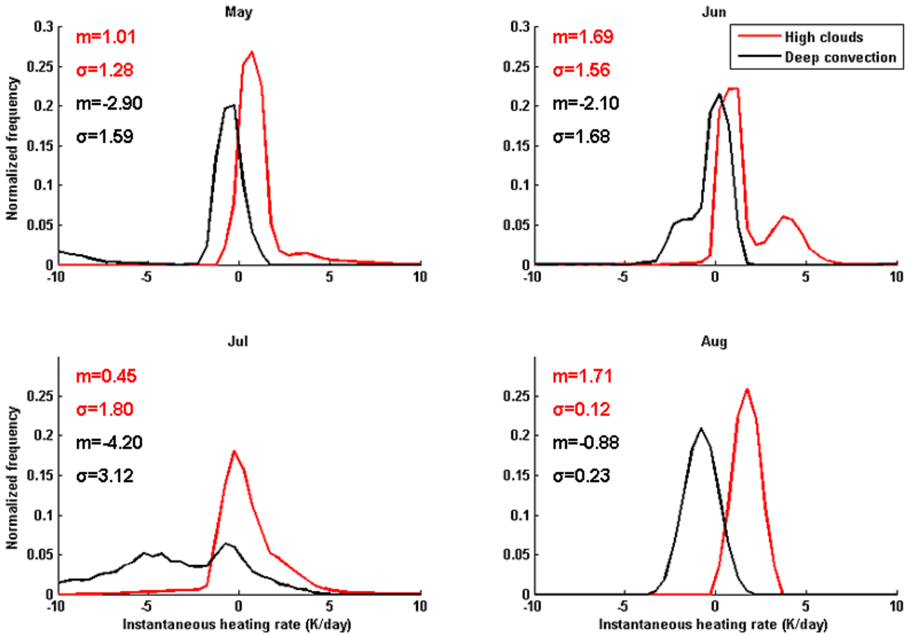

Figure 11. Probability density functions of instantaneous CRH for cloudy bins located above LZRH in all three regions (Z1–Z3) north of the equator for the years 2006–2010. The symbols m and σ denote mean and SD respectively.

ACPD
15, 5423–5459, 2015

Vertical structure of cloud radiative heating

E. Johansson et al.

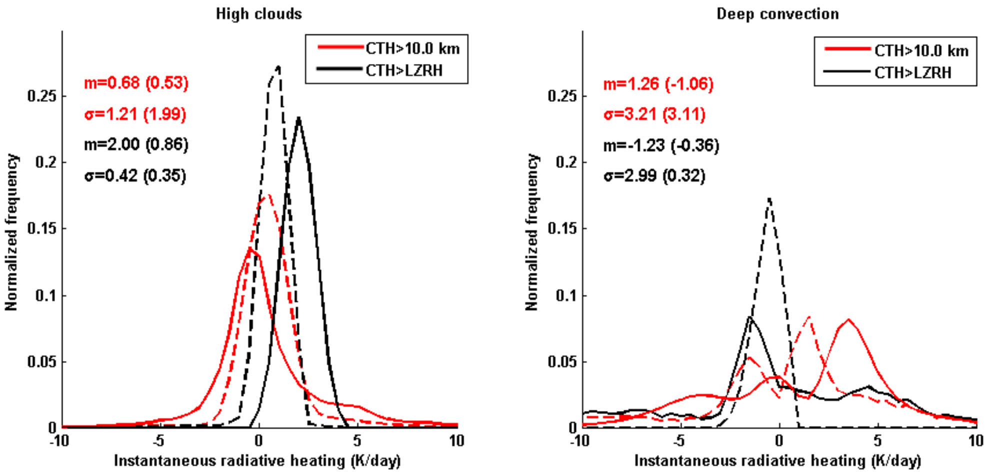

Figure 12. Probability density functions of instantaneous CRH for cloudy bins located above 10 km (red colour) and LZRH (black colour) during active and break periods of the monsoon. The solid lines show PDFs for active periods and dashed lines for break periods of the monsoon. The symbols m and σ denote mean and SD respectively. The values are for the break periods of monsoon.

ACPD
15, 5423–5459, 2015

Vertical structure of cloud radiative heating

E. Johansson et al.